Catal Lett (2008) 123:96–101
DOI 10.1007/s10562-008-9400-1

Temperature-programmed Studies of Coke Resistant Ni Catalyst for Carbon Dioxide Reforming of Methane

Yun-Xiang Pan · Chang-Jun Liu · Lan Cui

Received: 4 December 2007 / Accepted: 9 January 2008 / Published online: 23 January 2008

Abstract Argon glow discharge plasma was applied for drying the impregnated Ni/SiO_2 catalyst instead of the drying thermally. Such plasma treated catalyst significantly inhibits the coke formation from methane decomposition. The methane-derived carbon shows an improved reactivity against CO_2. This can result in a better balance of coke formation and gasification by CO_2 when the plasma-treated Ni/SiO_2 catalyst is used for the CO_2 reforming of methane.

Keywords Methane · CO_2 reforming · Ni/SiO_2 · Plasma · Coke resistance

1 Introduction

Carbon dioxide (CO_2) reforming of methane to synthesis gas attracts ever-growing interest from both environmental and industry aspects [1–6]. It provides a practical and effective way for the utilization of the two major greenhouse gases (CO_2 and methane) [2]. Many catalysts, including Ni-based catalysts and supported noble metal catalysts, show excellent activity for the CO_2 reforming of methane [7–11]. However, from the industrial standpoint of view, it is more practical to develop Ni-based catalysts due to the low-cost and the abundant resources of nickel.

A major problem of the Ni-based catalysts for the CO_2 reforming of methane is the continuous deactivation with time on stream due to coke formation. Methane decomposition is the major pathway for the coke formation at high temperature [9]. The methane-derived carbon can be gasified by CO_2, which is the primary way to eliminate the carbon. If the gasification of the carbon proceeds more slowly than the formation of the carbon, the carbon will deposit and deactivate the catalyst. The catalyst, on which the formation rate of the carbon is decreased or/and the gasification rate of the carbon is increased, is more favorable and more attractive for the CO_2 reforming.

Many efforts have been made to develop coke resistant Ni-based catalysts. One approach is the selective blockage of some of the Ni particle defect sites using inert element atoms [12–14]. This approach can lead to a good coke resistance, but it is usually accompanied by a decrease in the activity. Improving the preparation method for the catalysts is another approach [15–19]. For example, Tomiyama et al. [18] prepared a coke resistant Ni/SiO_2 catalyst for the CO_2 reforming by a process of homogeneous precipitation in wet gel.

Recently, we developed an argon glow discharge plasma technique for preparation of Ni-based catalysts for the CO_2 reforming [15–17]. Glow discharge is one of conventional non-thermal plasmas, which is characterized by high electron temperatures (10,000–100,000 K) and low gas temperatures (as low as room temperature) [20]. The energetic species (electrons, ions, and radicals) in the plasma can modify the metal particle sizes, the metal morphology and the metal-support interactions of the catalyst [21]. Such plasma-treated Ni-based catalysts show a significantly improved coke resistance for the CO_2 reforming of methane [15–17].

The purpose of this work is to better understand how the plasma treatment improves the coke resistance of the Ni/SiO_2 catalyst for the CO_2 reforming of methane. We firstly

---

Y.-X. Pan · C.-J. Liu (✉)
Key Laboratory for Green Chemical Technology of Ministry of Education, School of Chemical Engineering and Technology, Tianjin University, Tianjin 300072, P.R. China
e-mail: ughg_cjl@yahoo.com

L. Cui
Analysis Center, Tianjin University, Tianjin 300072, P.R. China

investigated the performance of the plasma-treated Ni/SiO_2 catalyst for the methane decomposition. Then, we characterized the methane-derived carbon via temperature programmed oxidation (TPO), temperature programmed hydrogenation (TPH) and CO_2 temperature programmed surface reaction (CO_2-TPSR) analyses. We will confirm that the plasma treatment suppresses the coke formation from methane decomposition and the methane-derived carbon on the plasma-treated catalyst is more reactive toward CO_2. A better balance of the carbon formation and gasification by CO_2 has been achieved. The coke resistance of the Ni/SiO_2 catalyst is thereby improved for the CO_2 reforming of methane.

2 Experimental

2.1 Catalyst Preparation

The Ni/SiO_2 catalyst (with 10 wt% of NiO) was prepared by incipient wetness impregnation method. The silica was commercially obtained ($S = 285$ m^2/g; Institute of Chemical Engineering, Tianjin, China). It was impregnated with the aqueous solution of nickel nitrate for about 12 h. The obtained sample was divided into two parts. One part was dried at 110 °C for another 12 h and then thermally calcined at 500 °C for 4 h. The other part was treated by the glow discharge plasma before further thermal calcination at 500 °C for 4 h. The plasma treatment apparatus has been shown elsewhere [17]. The sample (about 0.4 g) was loaded in a quartz boat and placed in the 'positive column' region of the glow discharge. When the pressure in the discharge tube was about 100 Pa, the glow discharge plasma was generated by applying 900 V to the electrode using a high voltage amplifier (Trek, 20/20B). The signal input for the high voltage amplifier was supplied by a function/arbitrary waveform generator (Hewlett Packard, 33120A) with a 100 Hz square wave. Ultra high pure grade argon (>99.999%) was used as the plasma-forming gas. The details of glow discharge plasmas have been described previously [20]. The discharge was initiated at room temperature without external heating or cooling. According to infrared temperature measurements (Icron 100PHT), the heating effect of the glow discharge can be ignored and the temperature of the catalyst powder was close to room temperature. Thermal calcination was then conducted with no use of glow discharge plasma. After calcination in air, both the samples were pressed, crushed and sieved through 40–60 mesh sieves before use. The samples with and without plasma treatment are denoted as P–Ni/SiO_2 and C–Ni/SiO_2, respectively.

2.2 Methane Decomposition

The methane decomposition was conducted in a quartz-tube fixed-bed reactor (i.d. 4 mm) under atmospheric pressure. It was carried out at 700 °C for 1 h. Before the reaction, the catalyst (50 mg, 40–60 mesh) was reduced at 500 °C for 2 h in flowing hydrogen at a flow rate of 50 mL/min. Then, methane was introduced into the reactor at a space velocity of 12,000 mL/(h gcat). The analysis of the effluent was carried out using an on-line gas chromatograph (Agilent 4890D) with a Porapak Q column and a thermal conductivity detector (TCD). The conversion of methane was calculated according to the following equations:

$$X(CH_4)\% = \left[(F_{CH_4,in} - F_{CH_4,out})/F_{CH_4,in}\right] \times 100\%,$$

where X and F represent the conversion and gas flow rate, respectively. After the methane decomposition, TPO, TPH and CO_2-TPSR analyses and transmission electron microscopy (TEM) observations were conducted over the used catalyst samples.

During the TPO analysis, the used catalyst sample was heated in flowing 3%O_2/He at 30 mL/min over the temperature range 50–1,000 °C at a heating rate of 10 °C/min. The CO ($m/z = 28$) and CO_2 ($m/z = 44$) signals were continuously recorded by an on-line quadrupole mass spectrometer (GSD301, Ommistar^{TM}). The CO_2 signals were calibrated by injecting known quantities of CO_2 into the gas stream. This calibration allows quantitative measurements of the carbon.

During the TPH analysis, the used catalyst sample was heated in flowing 5%H_2/Ar at 30 mL/min over the temperature range 50–1,000 °C. The heating rate was 10 °C/min. The methane ($m/z = 16$) signal was continuously recorded by the same mass spectrometer used for the above TPO analysis.

During the CO_2-TPSR analysis, the used catalyst sample was heated within the temperature range 50–1,000 °C at a heating rate of 10 °C/min. A gaseous mixture of CO_2 and helium (He) with a volume ratio of 1:3 was fed into the reactor at a flow rate of 40 mL/min. The CO ($m/z = 28$) and CO_2 ($m/z = 44$) signals were continuously recorded by the same mass spectrometer used for the above TPO analysis.

The TEM observations of the used catalyst samples were performed using a Philips TECNAI G^2F20 system. The samples were ground into fine powders and then ultrasonically dispersed in ethanol. A drop of the suspension was deposited on a carbon coated copper grid for the TEM analyses.

3 Results and Discussion

The fresh C–Ni/SiO_2 and P–Ni/SiO_2 samples have been investigated using the hydrogen temperature programmed

Table 1 Amount of the carbon on the used C–Ni/SiO_2 and P–Ni/SiO_2 samples after the CO_2 reforming of methane (700 °C, 4 h)

	C–Ni/SiO_2 sample	P–Ni/SiO_2 sample
Amount of the carbon (mg/gcat.)	45.1	22.0

Table 2 Changes of the conversion of methane over 1 h decomposition reaction at 700 °C

Conversion of methane			
	0 h	0.5 h	1 h
C–Ni/SiO_2 sample	26.3%	14.3%	5.4%
P–Ni/SiO_2 sample	11.7%	7.5%	6.7%

reduction (H_2-TPR), CO chemisorption, X-ray powder diffraction (XRD) and TEM observations in our previous work [17]. The plasma treatment enhances the interactions between the Ni particles and the silica. On the fresh P–Ni/SiO_2 sample, the size of Ni particles is smaller and the dispersion of the particles is more homogeneous.

The performances of the C–Ni/SiO_2 and P–Ni/SiO_2 samples for the CO_2 reforming of methane at 700 °C have also been evaluated [17]. At the beginning of the reaction, the activity of the P–Ni/SiO_2 sample is comparable to the C–Ni/SiO_2 sample. However, the P–Ni/SiO_2 sample shows an improved stability. The amount of the carbon on the used C–Ni/SiO_2 and P–Ni/SiO_2 samples after the CO_2 reforming, which are obtained via TPO analyses, is listed in Table 1. The TPO profiles of the used samples have been shown in the previous paper [17]. It is clearly seen that there is less carbon on the used P–Ni/SiO_2, indicating that this sample has an improved coke resistance for the CO_2 reforming of methane.

Table 2 shows the activities of the C–Ni/SiO_2 and P–Ni/SiO_2 samples at 700 °C for the methane decomposition. At the beginning of the reaction, the activity of the P–Ni/SiO_2 sample is lower than the C–Ni/SiO_2 sample. The conversion of methane on the C–Ni/SiO_2 and P–Ni/SiO_2 samples is 26.3% and 11.7%, respectively. Moreover, the deactivation rate of the C–Ni/SiO_2 sample is much higher than that of the P–Ni/SiO_2 sample. At 1 h, the conversion of methane on the C–Ni/SiO_2 sample is 5.4%, whereas it is 6.7% on the P–Ni/SiO_2 sample. A serious carbon deposition on the C–Ni/SiO_2 sample occurs. Further confirmation of the carbon deposition will be presented below with the TEM and TPO results.

Figures 1 and 2 show the TEM micrographs of the C–Ni/SiO_2 and P–Ni/SiO_2 samples after the methane decomposition at 700 °C for 1 h. In the TEM micrographs of the used C–Ni/SiO_2 sample, a large amount of carbon

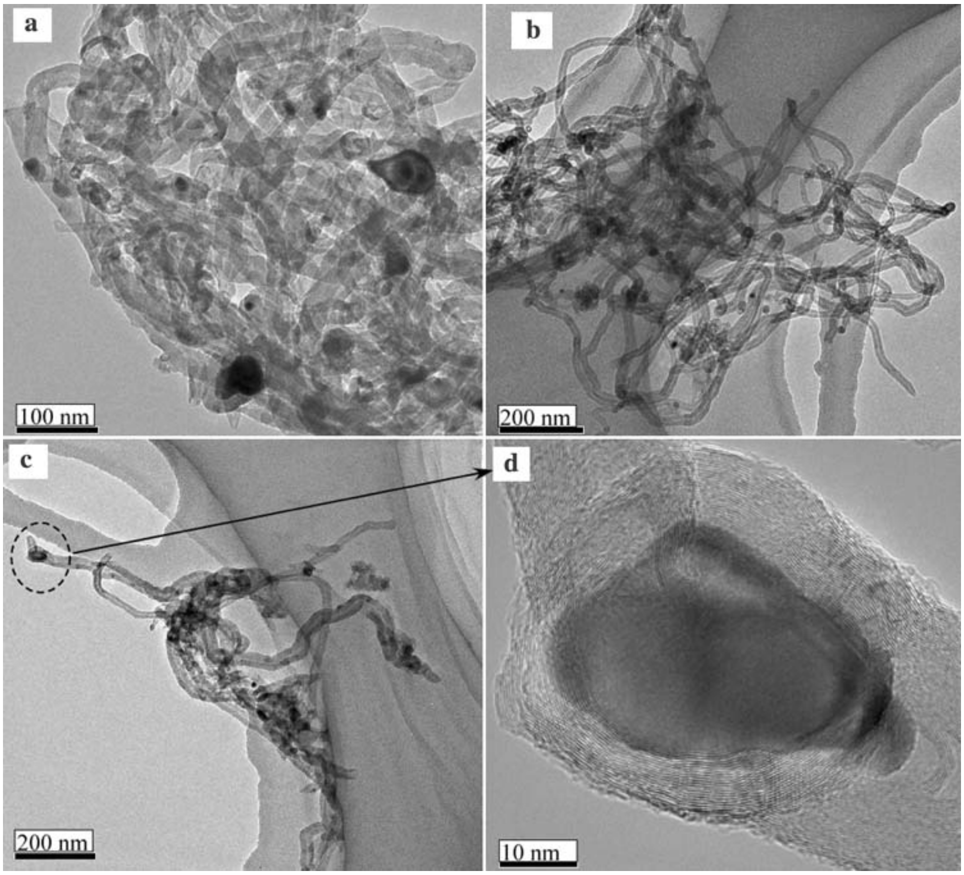

Fig. 1 TEM images of the used C–Ni/SiO_2 sample after the methane decomposition at 700 °C for 1 h

can be observed. Some Ni particles are encapsulated in the graphite sheets (Fig. 1c and 1d). Unlike the used C–Ni/SiO_2 sample, on the used P–Ni/SiO_2 sample, little carbon is observed. Furthermore, well-defined lattice fringes of the Ni(111) plane are observed on the used P–Ni/SiO_2 sample (Fig. 2c). The Ni particle with well-defined lattice fringes of the Ni(111) plane were also observed on the fresh P–Ni/SiO_2 sample, whereas more defects presented on the fresh C–Ni/SiO_2 sample [17]. Evidently, the amount of the carbon on the used P–Ni/SiO_2 sample is less than that on the used C–Ni/SiO_2 sample. This suggested that coke formation from the methane decomposition is suppressed on the P–Ni/SiO_2 sample.

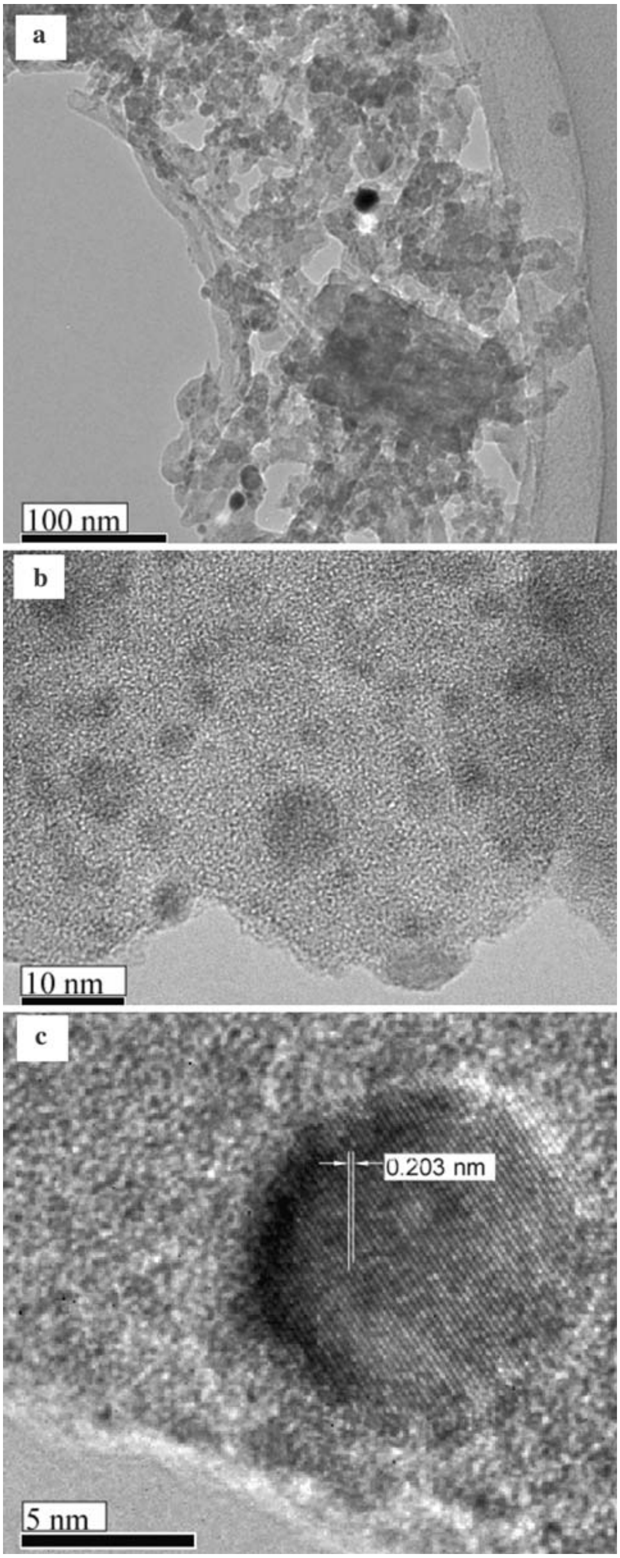

Fig. 2 TEM images of the used P–Ni/SiO_2 sample after the methane decomposition at 700 °C for 1 h

Figure 3 shows the TPO profiles of the used P–Ni/SiO_2 and C–Ni/SiO_2 samples after the methane decomposition. During the TPO analysis, no CO formation was observed. For the used C–Ni/SiO_2 sample, there are two main peaks located at 550 °C and 680 °C, whereas for the used P–Ni/SiO_2 sample the peaks appear at 525 °C and 680 °C. According to the literature [22], for both the used C–Ni/SiO_2 and P–Ni/SiO_2 samples, the lower temperature peak may be caused by the oxidation of filamentous carbon. The higher temperature peak for both the samples is probably generated from the oxidation of the graphite layers. For the C–Ni/SiO_2 sample, the amount of released CO_2 during the TPO analysis is found equal to 2.6 mmol/(gcat). So the amount of the carbon deposited on the C–Ni/SiO_2 sample during the decomposition reaction of 1 h corresponds to 31.2 mg/(gcat). For the P–Ni/SiO_2 sample, there are 1.5 mmol/(gcat) of CO_2 being released during the TPO analysis, indicating that the amount of the carbon deposited on this sample is 18.0 mg/(gcat). The amount of the carbon on the used P–Ni/SiO_2 sample is significantly reduced, which is agreement well with above TEM observations.

Wang et al. [22] and Ermakova et al. [23] have prepared filamentous carbon via methane decomposition on Ni/SiO_2 catalyst. These researchers suggested that catalyst with larger Ni particles and weaker interactions between Ni and

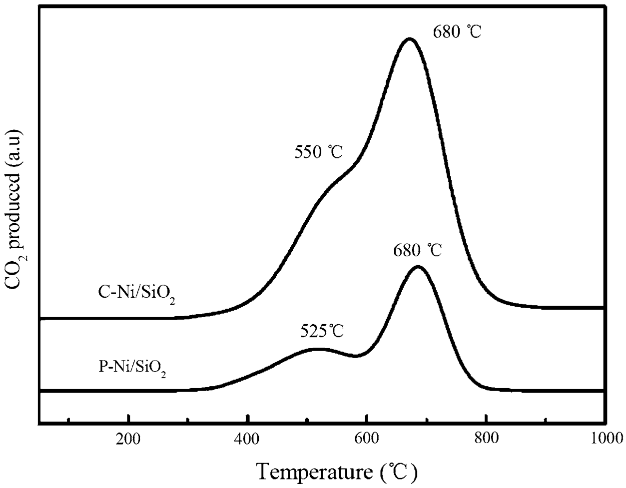

Fig. 3 TPO profiles of the used C–Ni/SiO_2 and P–Ni/SiO_2 samples after the methane decomposition at 700 °C for 1 h

silica are more favorable for the production of the carbon. Since the Ni particles of the P–Ni/SiO_2 sample are smaller and the interactions between Ni and the silica are stronger [17], it is not surprising that the coke formation from the methane decomposition is suppressed on this sample. In addition, well-defined lattice fringes of the Ni(111) plane are observed on the P–Ni/SiO_2 sample. However, on the C–Ni/SiO_2 sample, the Ni particle surface appears to be a complicated combination of many crystallographic planes [17]. This combination can cause high concentrations of distortions and lattice defects [24]. Methane decomposition is structure sensitive. Particles with close packed planes (such as Ni(111)) have higher activation energy than those with distortions and lattice defects [25–27]. This may be another reason for the suppression of the coke formation from methane decomposition on the P–Ni/SiO_2 sample.

For both the used C–Ni/SiO_2 and P–Ni/SiO_2 samples, there is only one peak in their TPH profiles (Fig. 4). For the used C–Ni/SiO_2 sample, the peak appears at 660 °C, whereas, for the used P–Ni/SiO_2, the peak presents at 615 °C. The initiative temperatures of the hydrogenation of the carbon on the used C–Ni/SiO_2 and P–Ni/SiO_2 samples are almost the same. This indicates that the carbon on both of the samples may have the same reactivity toward H_2. The TPH profile of the used C–Ni/SiO_2 sample is broader and less symmetrical, suggesting that there are different types of carbon on this sample. This is in agreement well with the TEM observations.

The CO_2-TPSR profiles of the used catalyst samples after the methane decomposition are shown in Fig. 5. For the used C–Ni/SiO_2 sample, a peak at 620 °C is observed. For the used P–Ni/SiO_2 sample, the peak is presented at 580 °C. For the used C–Ni/SiO_2, the initiative temperature of the CO_2 surface reaction is about 450 °C. For the used P–Ni/SiO_2, the CO_2 surface reaction starts at about 420 °C. These results show that the carbon deposited on the P–Ni/SiO_2 sample is more reactive than that on the used C–Ni/SiO_2 sample against CO_2. Therefore, on the P–Ni/SiO_2 sample, the carbon produced from methane decomposition can be more easily gasified by CO_2. The carbon amount by

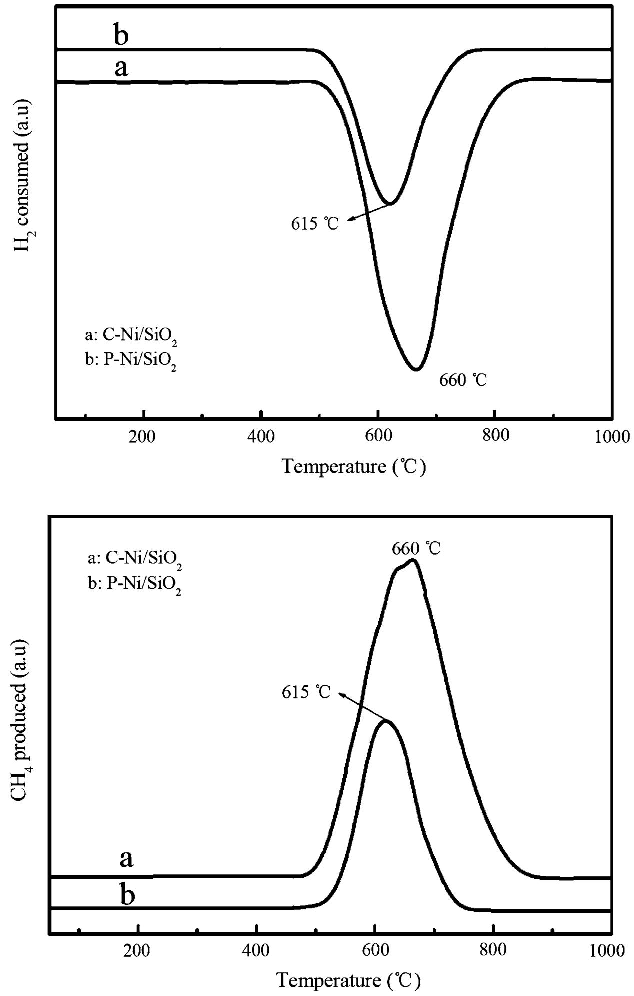

Fig. 4 TPH profiles of the used C–Ni/SiO_2 and P–Ni/SiO_2 samples after the methane decomposition at 700 °C for 1 h

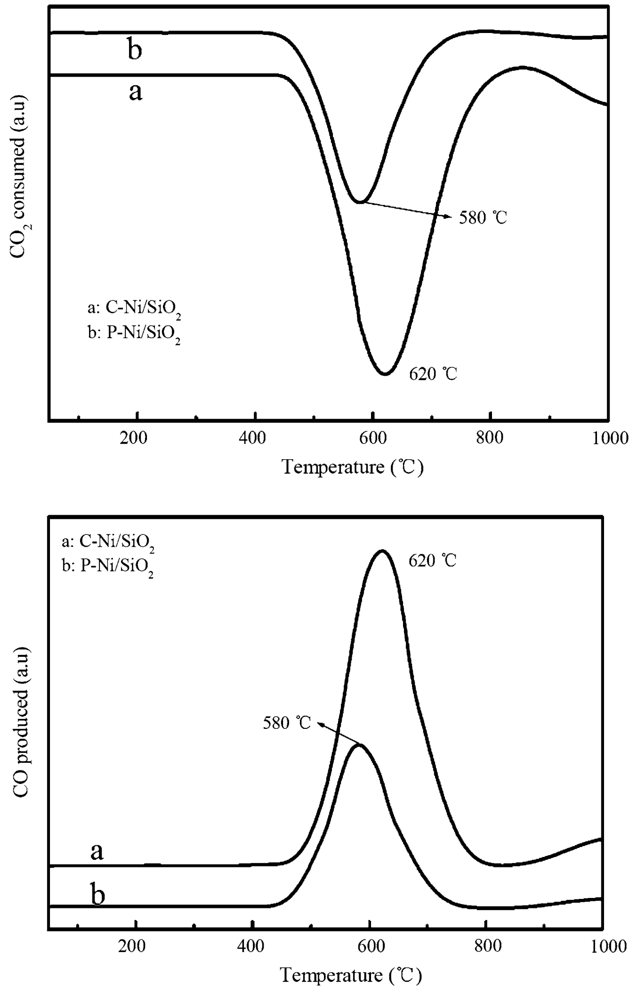

Fig. 5 CO_2-TPSR profiles of the used C–Ni/SiO_2 and P–Ni/SiO_2 samples after the methane decomposition at 700 °C for 1 h

integrating the CO_2-TPSR profiles is slightly lower than that estimated from the TPO results. There is about 91 wt% and 99 wt% of the carbon on the C–Ni/SiO_2 and P–Ni/SiO_2 samples reacting with CO_2, respectively.

4 Conclusion

Using an argon glow discharge plasma treatment technique, a coke resistant Ni/SiO_2 catalyst has been prepared for the CO_2 reforming of methane. On such plasma-treated Ni/SiO_2 catalyst, coke formation from the methane decomposition is suppressed. TEM and TPO results demonstrate that the methane-derived carbon on the plasma-treated Ni/SiO_2 catalyst is much less than that on the Ni/SiO_2 catalyst prepared by conventional impregnation method without plasma treatment. The CO_2-TPSR analysis indicates that the carbon on the plasma-treated Ni/SiO_2 catalyst is more reactive toward CO_2. Therefore, the methane-derived carbon is more easily eliminated by CO_2 on the plasma-treated Ni/SiO_2 catalyst. The suppression of the coke formation from methane decomposition and the higher reactivity of the methane-derived carbon against CO_2 can lead to an improved coke formation-gasification for the plasma-prepared Ni/SiO_2 catalyst when this catalyst is used for the CO_2 reforming of methane. This should be one of the reasons for the better coke resistance performance that the plasma-treated Ni/SiO_2 catalyst shows for the CO_2 reforming.

Acknowledgments The support from the National Natural Science Foundation of China (under contract 20490203) is greatly appreciated. The instruments supplied by ABB Switzerland and the support from the Program for Changjiang Scholars and Innovative Research Team from the Ministry of Education of China are also appreciated.

References

1. Hu YH, Ruckenstein E (2004) Adv Catal 48:297
2. Slade DA, Duncan AM, Nordheden KJ, Stagg-Williams SM (2007) Green Chem 9:577
3. Chen D, Lodeng R, Holmen A (2004) Stud Surf Sci Catal 147:181
4. Li XC, Li SG, Yang YF, Min W, Fei H (2007) Catal Lett 118:59
5. Chen D, Lodeng R, Anundskas A, Olsvik O, Holmen A (2001) Chem Eng Sci 56:1371
6. Liu BS, Li L, Au CT, Cheung ASC (2006) Catal Lett 108:37
7. Pompeo F, Nichio NN, González MG, Montes M (2005) Catal Today 107–108:856
8. Ross JRH (2005) Catal Today 100:151
9. Wang ZJ, Zhao Y, Cui L, Du H, Yao P, Liu CJ (2006) Green Chem 9:554
10. Wang SB, Lu GQM (1996) Energy Fuels 10:896
11. Wang SB, Lu GQM (1998) Appl Catal B 16:269
12. O’Connor AM, Schuurman Y, Ross JRH, Mirodatos C (2006) Catal Today 115:191
13. Nikolla E, Holewinski A, Schwank J, Linic S (2006) J Am Chem Soc 128:11354
14. Sun H, Wang H, Zhang J (2007) Appl Catal B 73:158
15. Zhu XL, Zhang YP, Liu CJ (2007) Catal Lett 118:306
16. Cheng DG, Zhu XL, Ben YH, He F, Cui L, Liu CJ (2006) Catal Today 115:205
17. Pan YX, Liu CJ, Shi P (2007) J Power Sources (in press; doi:10.1016/j.jpowsour.2007.10.039)
18. Tomiyama S, Takahashi R, Sato S, Sodesawa T, Yoshida S (2003) Appl Catal A 241:349
19. Che M, Cheng ZX, Louis C (1995) J Am Chem Soc 117:2008
20. Liu CJ, Vissokov GPB, Jang WL (2002) Catal Today 72:173
21. Zou JJ, Liu CJ, Zhang YP (2006) Langmuir 22:2334
22. Wang P, Tanabe E, Ito K, Jia J, Morioka H, Shishido T, Takehira K (2002) Appl Catal A 231:35
23. Ermakova MA, Ermakov DY (2002) Catal Today 77:225
24. Kroll VCH, Swaan HM, Mirodatos C (1996) J Catal 161:409
25. Choudhary TV, Goodman DW (2000) J Mol Catal A 163:9
26. Burghgraef H, Jansen APJ, Santen RAV (1995) Surf Sci 324:345
27. Rostrup-Nielsen JR, Nørskov JK (2006) Top Catal 40:45